Paper No.
00070

CORROSION 2000

CORROSION INHIBITION OF WET GAS PIPELINES UNDER HIGH GAS AND LIQUID VELOCITIES

Michael Swidzinski
Phillips Petroleum
35 Guildford Road, Woking
Surrey GU22 7QT, UK

Bob Fu and Audrey Taggart
Nalco/Exxon Energy Chemicals, L.P.
7705 Highway 90-A
Sugar Land, Texas 77478, USA

W. Paul Jepson
Corrosion in Multiphase Systems Center
Department of Chemical Engineering, Ohio University
Athens, OH 45701, USA

ABSTRACT

Work was conducted to assess the applicability of carbon steel pipeline and corrosion inhibitor as a viable combination for transporting wet multiphase corrosive petroleum fluids under high gas and liquid velocities. Flow loop tests were performed to study the performance of inhibitors under simulated field conditions with gas and liquid velocity as high as 25 m/s. The results showed that inhibition efficiency greater than 96% can be achieved with 100 to 200 ppm of corrosion inhibitors specially formulated for high shear applications. The performance of inhibitors with respect to concentration showed a typical profile similar to that observed at lower velocity. The effective concentration was dependent upon the flow regime. Slug flow typically required a higher concentration due to its severe flowing condition. The positive results support the combined use of carbon steel and corrosion inhibition as a viable and cost-effective option for the development of a pipeline system for the transportation of wet corrosive multiphase hydrocarbon fluids at high velocity.

Keywords: wet gas, CO_2 corrosion, high velocity, corrosion inhibition, and inhibitors

INTRODUCTION

As more and more energy reserves have been discovered in remote areas, such as in deepwater offshore, it has become increasingly challenging to efficiently produce the petroleum fluids from these remote locations. One major challenge is to transport these "*unprocessed*", multiphase fluids from the remote area to the central processing facility safely and cost effectively. In order to assure an uninterrupted flow of fluids, or ultimately the flow of revenues, the operator must inhibit any deposition of solids, such as scales, hydrates, waxes and asphaltenes, while maintaining the integrity of the production system by minimizing corrosion and/or erosion. This paper is to address the issues related to corrosion and inhibition of pipelines carrying high velocity gas or liquids.

Carbon dioxide corrosion in wet gas pipelines is a well-known phenomenon.[1-4] Extensive studies have been carried out in order to better understand the corrosion mechanisms.[5-7] These studies were often conducted in laboratories where a much smaller scale system, such as high-pressure flow loops, was built to simulate the real life system.[8-10] A number of test protocols have also been developed for these simulation systems. The resulting experience had contributed to significant improvement in corrosion control and mitigation for the past two decades. These laboratory scale systems not only were used to assess the severity of corrosion, quite often they were also used as the screening tools for selection of corrosion inhibitors.[10-15]

In the production and transportation of petroleum fluids from remote locations, multiphase flow is often encountered and a range of different flow regimes can be experienced in pipelines. For example, the flow regimes can be stratified, slug or annular in horizontal and slightly inclined pipelines. The predominant flow regime is determined by the flow rates and gas/liquid ratio. The wall shear stress associated with these flow regimes, particularly slug flow, is very different from those in the single-phase flow.[5] Despite the advances in the past few decades, the effect of flow on corrosion is not completely understood, especially when multiphase flow is involved.[16-18]

Most laboratory tests have been carried out in small diameter (< 5 cm) single-phase flow systems using actual or synthetic fluids. The effect of wall shear stress in these systems shows a general trend of increasing corrosion rate with increasing liquid velocity and hence increasing shear stress. Inhibitors have been shown to provide good corrosion protection in these systems, which can generate shear stress as high as 300 Pa. However, study of corrosion in multiphase flows requires a more sophisticated multiphase flow simulator. A much higher shear stress can be generated in slug flow due to tremendous turbulence at the front of the slug. At slug front gas bubbles are entrained in the liquid and forced towards the bottom of the pipe where they impact and sometimes collapse on the wall, resulting in instantaneous high shear on the wall. Values as high as 3000 Pa have been recorded in the authors' laboratory.[1] When evaluating corrosion inhibitors, it is important to consider all of these flow effects that might exist in the multiphase pipelines.

This work was initiated to assess the viability of using the combination of carbon steel and corrosion inhibitor as the design base for the construction of a multiphase pipeline. The pipeline will be used to transport wet gas from a new development located in the North Sea. The diameter of the pipeline must be carefully sized in order to achieve the maximum throughput without causing excessive corrosion and erosion resulting from high fluid velocities. Higher throughput is preferred because of the

[1] The values were recorded when the slugs were passing by the hot film probe.

advantage of having higher production rates and lower liquid holdups. However, higher fluid velocity generates higher wall shear stress that can be detrimental to the inhibitor film on the surface. It is believed that there exists a velocity limit above which the inhibitor film is likely be stripped from the surface.[20-22] The challenge to the design engineers is to find the optimum pipeline dimension that offers the highest throughput while keeps the fluid velocity below the safe limit. The inhibitor film remains stable on the surface under this limit.

In this study, the corrosiveness of petroleum fluids under selected, severe flowing conditions was established and the ability of inhibitors to mitigate the flow enhanced corrosion was investigated Two corrosion inhibitors, A and B, that have been specifically formulated for high velocity applications were evaluated in this study. Inhibitor A is a polyamidoamine-based formulation and inhibitor B is an imidazoline-based blend. The work was carried out in two high-pressure flow loops, one single-phase and the other multiphase. The single-phase flow loop was used for the study of high liquid velocity and the geometrical effect. The multiphase flow loop was used to study high gas velocities and the flow regime effect.

EXPERIMENTAL

Single-phase Flow Loop Study

The single-phase flow loop used in this study is a 2.54-mm closed loop that has three parallel test sections. The schematic of this loop is shown in FIGURE 1. The details of this loop and its operation are published elsewhere.[9]

The test specimens were machined from a pipe section of API X-65 grade. Specimens of two different shapes were used in the experiments. The ring-type specimens (dimension: 6.4 mm ID x 9.5 mm length) were used for the flow-through probe. The tube-shape specimens (dimension: 5 mm OD x 45 mm length) were used for the elbow and dead leg probes. The surface-to-volume ratio was about 1 cm^2 metal surface per 1075 cm^3 fluid. Prior to each test, the specimens were pre-conditioned by being sandblasted with 60-100 mesh amorphous glass beads. The specimens were then sonically cleaned in acetone, rinsed with isopropanol, dried and weighed, before being mounted on the probe. A total of three probes, each mounted in a different geometrical location, were used in each test. Corrosion rates were measured using LPR (linear polarization resistance) technique as well as weight loss method.

Following each test, the specimens were removed, dried, and immersed in an inhibited acid for 5 minutes. The inhibited acid was a 2:2:1 mixture of acid:water:commercial corrosion inhibitor. The electrodes were then removed, cleaned with soap and steel wool, and dried. Isopropanol was then used to rinse off any organic residues before the electrodes were weighed for weight loss measurement.

The test fluid consisted of the synthetic brine and a hydrocarbon solvent (a hydrotreated light paraffinic distillate). The brine to hydrocarbon ratio was 9:1. The liquid velocity ranged from 2 to 14 m/sec. The temperature and pressure were fixed at 93°C and 0.8 MPa, respectively. The flow loop was under a CO_2 blanket throughout the test to simulate the sweet condition. The oxygen content was measured after each test to be less than 5 ppb. The composition of the synthetic brine, listed in TABLE 1, was based on the water analysis from a test well.

TABLE 1. The composition of the synthetic brine used in the flow loop study

Ionic Species	Na^+	Ca^{2+}	Mg^{2+}	Ba^{2+}	Sr^{2+}	HCO_3^-	SO_4^{2-}	Cl^-
Concentration, ppm	49,047	9,270	795	230	800	245	9	95,670

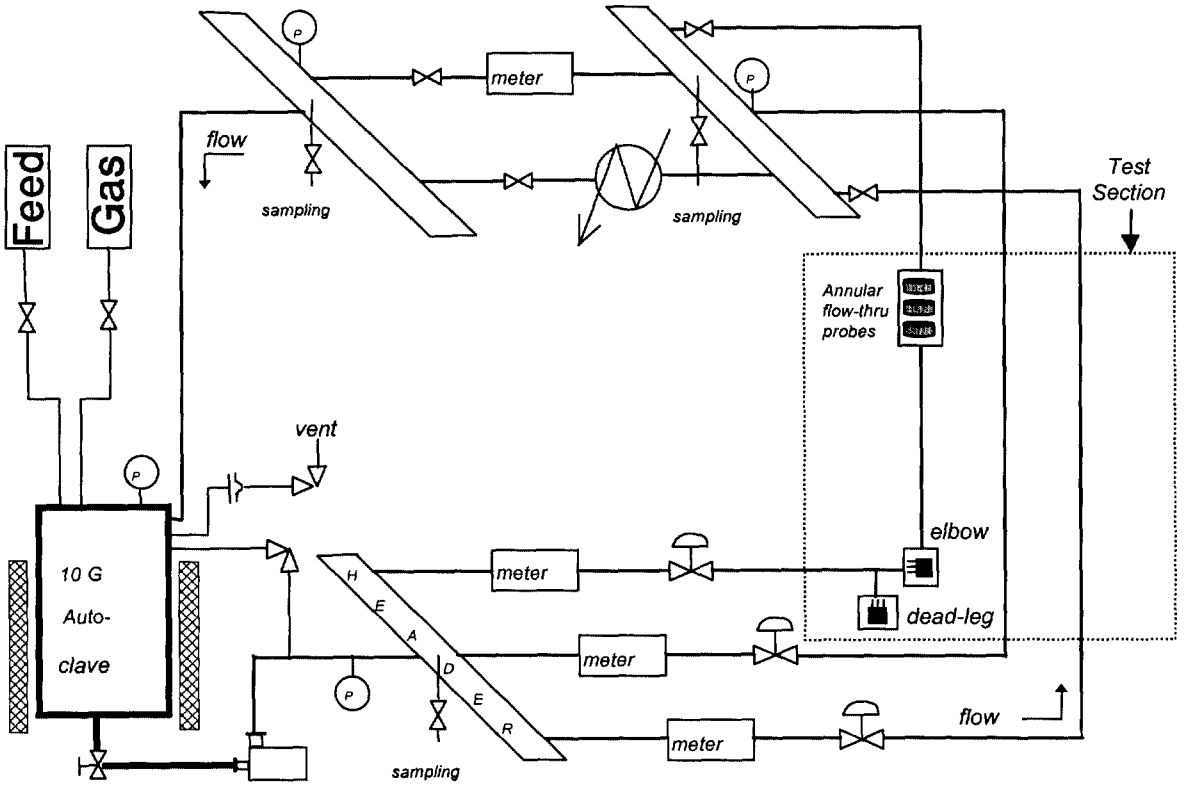

FIGURE 1. The schematic diagram of the high pressure single-phase flow loop

Multiphase Flow Loop Study

The multiphase flow loop is a 10.2-mm high-pressure loop that can be operated at pressure up to 17.2 MPa and temperature up to 140°C. This 316L stainless steel loop is equipped with a 1.4 m^3 HP (high pressure) vessel and a progressing cavity pump, in addition to various instrumentation for flow control and corrosion measurement. The HP vessel served as the reservoir for the recirculation of fluids as well as a separator for separating the returning multiphase (a gas-oil-water mixture) fluids. The progressing cavity pump is capable of driving the wet gas stream to high velocities up to 30 m/s. The loop can be lifted to any inclination up to 90° vertically. The test section, 2 meters in length, is located in the center of a 18-meter long straight section. The test temperature was controlled by flowing heated oil, with its temperature and flow rate properly regulated, through the outer jacket of the HP reservoir. The schematics of the multiphase flow loop and its test section are shown in FIGURE 2 and 3, respectively.

Shear Stress Determination

Shear stress was either measured directly using a commercially available hot film probe or estimated from the physical parameters used in the experiments. The equation used for calculating the shear stress in a straight pope section (applicable to the flow-through probe) is shown as follows,

$$\tau = (f_D * \rho * v^2) / (8 * g) \qquad \text{Eq. (1)}$$

which,

τ:	shear stress
f_D:	Darcy friction factor
ρ:	density
v:	velocity
g:	gravitational constant.

The Darcy friction factor, f_D, was calculated based on the Colebrook equation shown below.[23]

$$\frac{1}{\sqrt{f_D}} = -2\log\left[\frac{e/D}{3.7} + \frac{2.51}{Re\sqrt{f_D}}\right] \qquad \text{Eq. (2)}$$

which,

e:	surface roughness
D:	pipe diameter
Re:	Reynold's number (=$D v \rho / \mu$; μ is the viscosity)

The shear stress at the elbow was estimated to be three times the value found in the straight section. This ratio was established through many testing in the authors' laboratory.

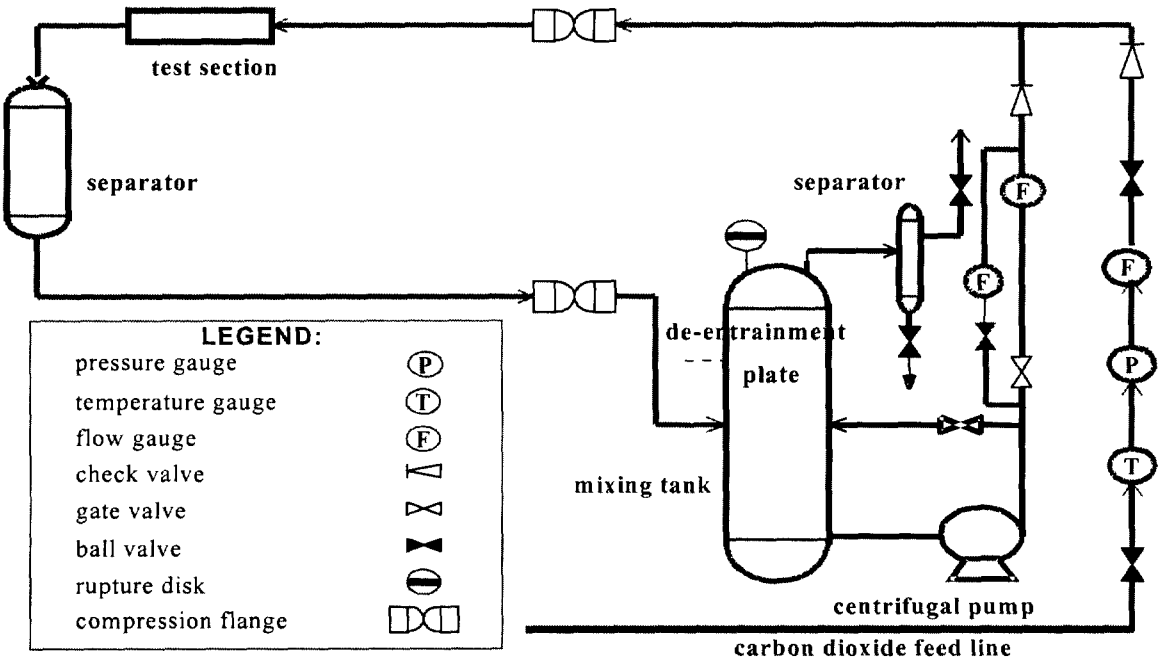

FIGURE 2. The schematic of high pressure multiphase flow loop

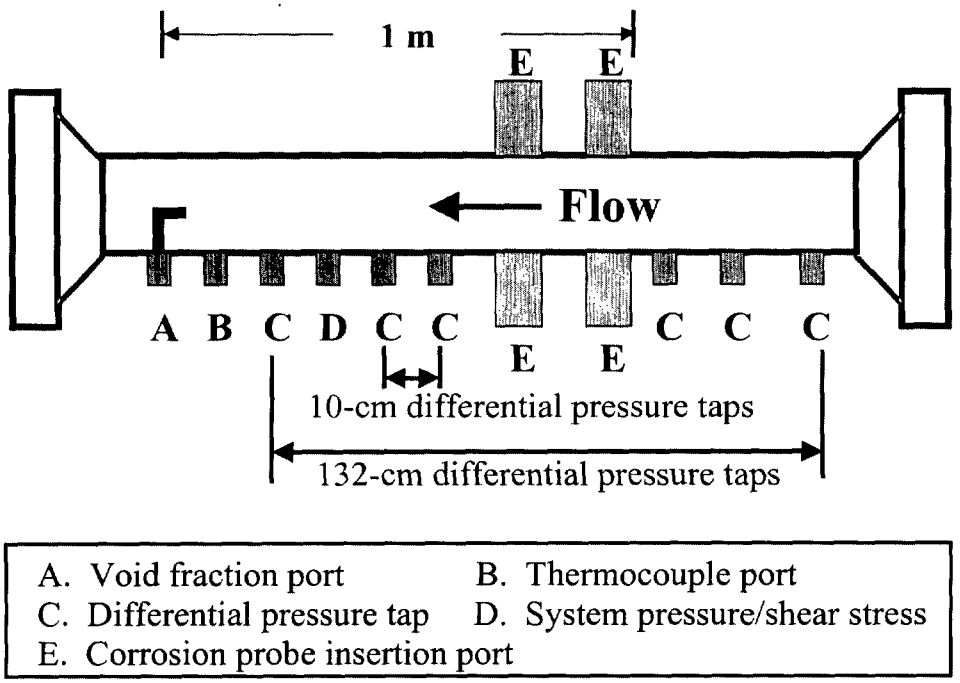

FIGURE 3. The test section in the high pressure multiphase flow loop

At the start of each experiment, a predetermined amount of oil and water was fed into the reservoir. The water and hydrocarbon liquids were moved through the system by a 3-15 kW centrifugal pump. The liquid flow was metered with an inline turbine meter and was controlled at a rate of 50 to 100 m^3/hr using a variable speed drive and a by-pass stream. Carbon dioxide was fed to the loop at 2-MPa pressure from a storage tank containing 25,000 kg of gas. The gas feed line was used to pressurize the loop as well as to calibrate the system at the initial startup. A vent line with a back pressure regulator and a knock out drum was used to bleed the excess gas from the system when required. As soon as the desired gas velocity was reached, the vent line was closed to begin the recirculation of gas. The liquid pump was then turned on and tuned to the liquid velocity corresponding to a GOR (gas-to-oil ratio) of 1780 sm^3/sm^3. The liquids then mixed with the recirculating gas and the resulting multiphase fluids passed through the test section. The multiphase fluids were continuously circulated at the specified flow rate by the progressing cavity pump that used a variable speed drive and a reduction gear system to maintain the required flow rate.

The test section contains two pairs of access ports, located evenly at the top and the bottom of the pipe. Two commercial ER probes, one fitted with conventional mass loss technique and the other with inductance resistance technique, were flush mounted to collect corrosion rate data. The ER probe has the wire element embedded in a flush-mount design. The specimens for weight loss measurement were 1 cm in diameter and 3 mm thick. The surface-to-volume ratio was so large to be of no concern.

The actual gas velocity was measured using a Pitot tube mounted in the test section. A sampling tube was used to determine the concentration of oxygen and ferrous ion in the system. A pH probe was also installed to monitor the *in-situ* pH. While the Pitot tube was mainly used for measuring the gas velocity, it was also utilized for counting the number of slugs when slug flow existed. Slug frequency was monitored by examining the pressure responses from the Pitot tube.

Gas velocities of 7.5, 15, and 25 m/s were used at a GOR of 1780 sm^3/sm^3. Either slug or annular flows existed under these conditions. All tests were carried out at a system pressure of 0.8 MPa using carbon dioxide and temperatures of 95 and 130°C. The baseline corrosion rate without any corrosion inhibitors was measured first. Corrosion inhibitor was then added at 50 ppm increment based on the total liquid in the system. The experiments were repeated to determine the effectiveness of the inhibitor at various concentrations up to 200 ppm. The test matrix in the multiphase flow loop study is listed in TABLE 2.

TABLE 2. The test matrix used in the multiphase studies

Test Parameters	Condition
Partial pressure of carbon dioxide	0.8 MPa
Temperatures	95 and 130°C
Gas velocities	7.5, 15, and 25 m/s
GOR (gas-to-liquid ratio)	1780 sm^3/sm^3
Liquid 1	90% synthetic brine and 10% oil
Liquid 2	100% de-ionized water
Liquid 3	90% de-ionized water and 10% oil
Oil:	hydrotreated light paraffinic distillate, 2 cP @ 40°C
Inhibitor	A and B
Concentration	50, 100, 150, 200 ppm

RESULTS AND DISCUSSIONS

Single-phase Flow Loop Study

Corrosion probes were mounted in three different locations, namely elbow, dead leg and a straight section, in the loop. This was to simulate the condition at various geometrical locations that may be present in the pipeline. The baseline corrosion rate with respect to time was established first. A typical profile is shown in FIGURE 4. In general, the highest corrosion rate was obtained from the flow-through probe (mounted in the straight section) and the lowest was found in the dead leg probe. This trend followed the same order as the flow severity expected in these geometrical locations. The flow severity should be higher at the elbow than in the straight section under the same flow rate (1.58 L/s in blank test #1 and #2). However, since the pipe ID at the elbow (35 mm) was much larger than that in the flow-through probe (12.7 mm), the flow severity and consequently the measured corrosion rates were higher in the straight section. The ID was intentionally made larger at the elbow in order to accommodate the corrosion probe. As shown in FIGURE 4, the corrosion rates measured in all locations were reasonably stable after a short initial period.

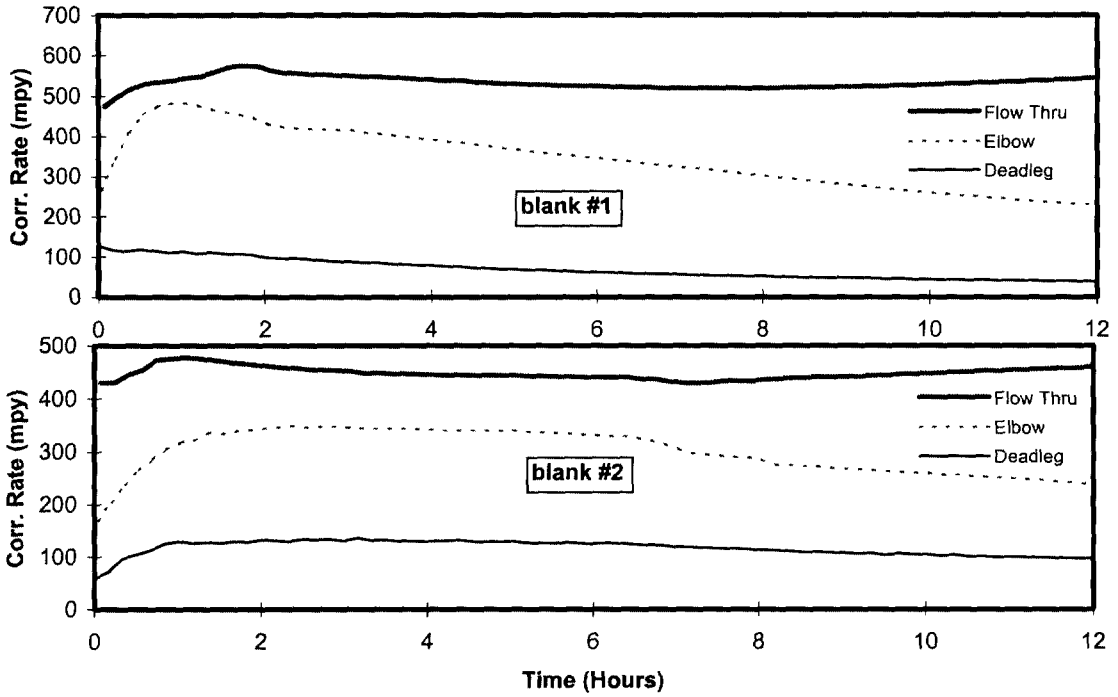

FIGURE 4. The profile of baseline corrosion rates with respect to time

In addition to the dependence on the geometrical locations, the baseline corrosion rate also varied from one test to the other. For example, the corrosion rate acquired from the flow-through probe ranged from 500 mpy to 700 mpy when the 12.7-mm ID specimens were used. The liquid flow rate through the 12.7-mm ring specimens in the flow-through probe was 1.58 L/s. This was equivalent to a linear velocity of 12.5 m/sec with an estimated shear stress of 550 Pa. Some of the observed data scattering was likely caused by the scaling of the synthetic brine that contained a significant amount of calcium, barium and strontium ions.

Two specially formulated inhibitors, A and B, were evaluated under these severe flowing conditions. In the inhibitor study, the ID of 12.7-mm rings in the flow-through probe was further reduced to 6.4-mm and the other two probes were mounted on a separate test section. These changes were made to enhance the flow severity. The liquid velocity was thereafter raised to 14 m/s with corresponding shear stress increased to 850 Pa. The velocity at the elbow was also slightly increased but was much lower at 2.2 m/s with estimated shear stress of 42 Pa. Since the absolute corrosion rates can vary from one test to the other, it was decided to compare the performance of inhibitors at various concentrations based on the degree of protection. The test protocol called for establishing the stable baseline corrosion rate first before a predetermined concentration of inhibitor was injected. The corrosion protection was then calculated based on the individual baseline corrosion rate measured from each experiment. The performance of inhibitor A and B is shown in FIGURE 5 and 6, respectively.

The corrosion inhibition effect was immediately noticed upon the injection of inhibitors. This reflected the unique characteristic of fast adsorption kinetic and the formation of a strong protective film from both inhibitors. Corrosion on the dead leg and elbow probes was effectively inhibited at 50 ppm of

inhibitor A. A higher concentration of 100 ppm was required for the flow-through probe where the flowing condition was the most severe. The efficiency of inhibition can be slightly improved by increasing the corrosion inhibitor concentration. Indeed, corrosion protection greater than 97% was accomplished by applying 200 ppm of inhibitor A. The performance of inhibitor B was very similar to that observed for inhibitor A. Again, 50 ppm of inhibitor B was required to inhibit corrosion on the dead leg and elbow probes. The flow-through probe required 200 ppm to achieve 90% corrosion protection. Corrosion protection greater than 97% is expected for all three probes in the presence of 200 ppm of either inhibitor.

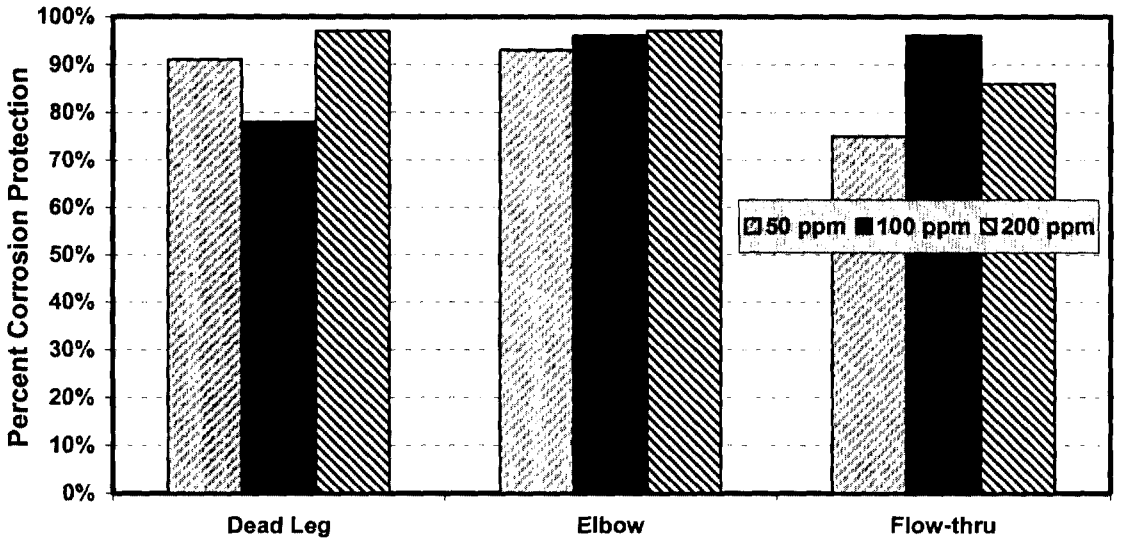

FIGURE 5. The performance of inhibitor A at various concentrations and locations

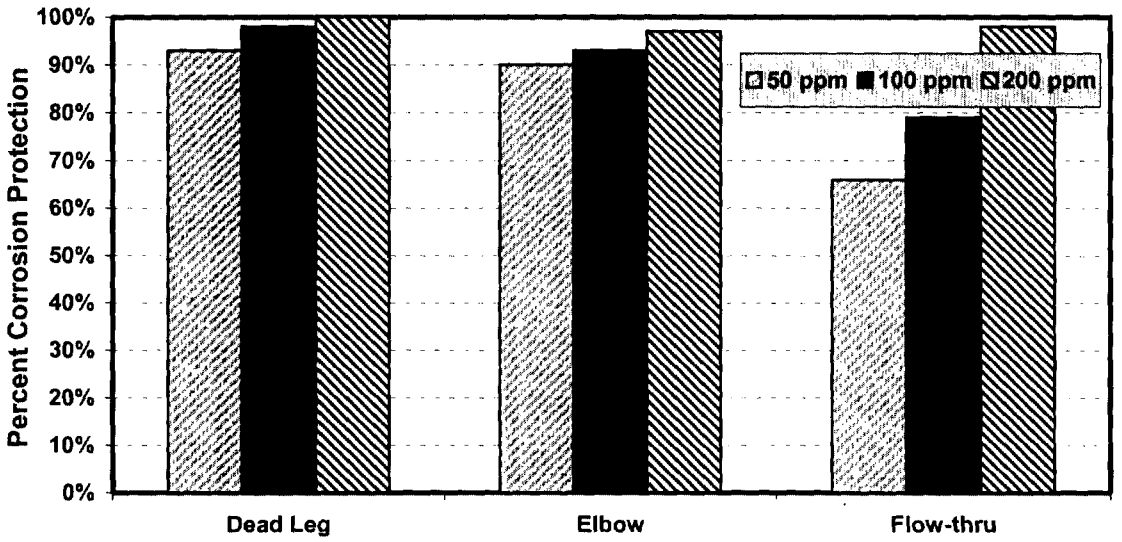

FIGURE 6. The performance of inhibitor B at various concentrations

It was noted that the corrosion protection on the dead leg probe at 100 ppm of inhibitor A (in FIGURE 5) was unusually low with only 78% protection. The low efficiency was attributed to the low baseline corrosion rate (25 mpy) obtained in this particular experiment. This led to low percentage of protection despite the fact that the final corrosion rate was merely 5 mpy. For comparison, the typical corrosion rate at the elbow was greater than 400 mpy. It is thought that scale deposit on the dead leg probe, where the fluid is relatively stagnant and thus conducive to deposition, may have been responsible for the low baseline corrosion rate. Indeed, presence of scales was verified by visual inspection following the test. Scales were not presence at all tests and hardly appeared in the inhibitor tests due to lower solution pH compared to the baseline runs.

The low baseline corrosion rate was also responsible for the lower-than-expected 86% protection on the flow-through probe with 200 ppm of inhibitor A. Under normal circumstance, corrosion protection greater than 95% should be expected at this concentration. In fact, corrosion protection of 96% has already been achieved in a previous test using a lower concentration (100 ppm). The baseline corrosion rate was only 400 mpy in this experiment, as compared to the typical corrosion rate that was at least twice higher. The fact that the inhibited corrosion rate at 200 ppm was comparable to that obtained at 100 ppm, both around 50 mpy, suggests that inhibitor A performed well at either concentration. It is interesting to point out that even the probe at the highest shear location cannot be spared from fouling due to scale deposition. This is consistent with the scale formation mechanism in pipeline conditions.

The corrosion rates reported in this section were acquired from the LPR probes. These corrosion rates were also verified by the weight loss method. The corrosion rates determined from the weight loss of the electrodes were generally higher than those measured by the LPR technique. However, the trend remains the same regardless of the absolute corrosion rates. It is believed that the reported corrosion rates are slightly smaller than the actual rates. The Stern-Geary constant (B value) used in the current-to-rate conversion is 26 mV,[24,25] which is likely smaller than what it should be. The actual Stern-Geary constant was not measured due to the difficulty and uncertainty involved.

Multiphase Flow Loop Study

Corrosion and Inhibition Using Synthetic Brine and Oil. As shown in TABLE 2, the initial experimental design was to include gas velocities of 7, 15, and 25 m/s and test temperature of 95 and 130°C in the matrix, using a synthetic brine and oil. These values were chosen in order to simulate the expected field conditions. However, slight variations were made during the course of the tests in order to adjust for the limitations and difficulties that were later encountered in the experiments.

One difficulty was experienced with the new multiphase pump when the temperature was raised to 90°C. The test temperature was too high for the rotor of the pump. The high temperature caused significant thermal expansion of the rubber in the stator. As a consequence, the stator became too tight for the rotor to fit. The rubber began to be stripped from the stator after a period of 24 hours. This led to high levels of vibration and contamination in the system, especially at higher gas velocities. Furthermore, the efficiency of the pump decreased with time and eventually the pump failed. The baseline tests were completed before the pump failure and tests were repeated to reconfirm the results after a new stator was installed. The new pump assembly limited the test temperature to 95°C in order to achieve the high gas velocity at 23 m/s. The test results are summarized in TABLE 3 below.

TABLE 3. Baseline and inhibited corrosion rates at 95°C and 0.8 MPa CO_2 in multiphase flow containing 90% synthetic brine and 10% oil as liquid phase

Gas velocity, m/s	Baseline corrosion rate, mpy	Inhibitor dosage ppm	Corrosion rate after 1 hr, mpy	Corrosion rate after 2 hr, mpy	Corrosion rate, final mpy	Percent protection
7.5	105	50	skipped*	skipped*	skipped*	N/A
7.5	105	100	23	17	16	85%
7.5	105	150	16	12	11	90%
7.5	105	200	10	10	10	91%
15	67	50	skipped*	skipped*	skipped*	N/A
15	67	100	6	3	< 2	97%
15	67	150	skipped[&]	skipped[&]	skipped[&]	N/A
23	45	50	19	14	14	69%
23	45	100	3	< 2	< 2	96%
23	45	150	skipped[&]	skipped[&]	skipped[&]	N/A

* The test was unnecessary judging from the low corrosion protection at 23 m/s gas velocity and 50 ppm inhibitor.
[&] The test was unnecessary because corrosion was successfully inhibited at the lower velocity.

It was noted that the flow regime depended heavily on the gas velocity. The predominant flow regime was slug flow at gas velocity of 7.5 m/s and changed to annular flow at gas velocities of 15 m/s and higher. Since slug flow generated the highest flow turbulence, the corrosion rate measured was the highest at 7.5 m/s gas velocity. It was also noted that the corrosion rate was higher at 15 m/s gas velocity (67 mpy) than at 23 m/s (45 mpy). This phenomenon was not unusual and has been observed in other studies conducted in the authors' laboratory. It can be explained by a combination of two effects. In annular flow, an increase in the gas velocity can result in more liquid entrainment in the gas phase and more spreading of the remaining liquid around the pipe. Both effects lead to the thinning of the liquid film and consequently the average velocity in the boundary layer in the remaining liquid film can be lower, resulting in a lower corrosion rate.

The corrosion rate measurements were taken using both types of ER probes. The inductance type of probe is more sensitive than the conventional type and therefore data were taken every 5 minutes from the former and every 15 minutes from the latter. The corrosion rates obtained from both probes were comparable to each other, typically within 10-15 mpy in difference. If the difference was larger than this average, the experiment was repeated. Some later experiments were performed using two inductance ER probes to improve the response time. Each test was not terminated until a steady state corrosion rate has been recorded for at least an hour.

Although the multiphase flow loop is constructed of 316L stainless steel, the multiphase pump did produce a small amount of ferrous iron, Fe^{++}. The iron concentration ranged from 20 ppm (in the baseline experiments) to 50 ppm (in the inhibitor experiments). Since the saturation level of Fe^{++} in the solution is expected at much higher value (*i.e.,* greater than 130 ppm Fe^{++}), this small amount of iron did not appear to interfere with the experiments. In fact, pH was found to be stable at approximately 4.8. An excess amount of iron in the solution would raise pH to above 5 readily.

The baseline corrosion rate increased with decreasing gas velocity. The increase in corrosion was marginally when gas velocity was decreased from 23 to 15 m/s (from 45 to 67 mpy). However, a nearly two-fold increase was observed when the gas velocity was further reduced to 7.5 m/s (from 67 to 105 mpy). The pronounced effect was attributed to the change of flow regime from annular flow to slug flow, which resulted in more severe flowing condition.

Only inhibitor B was evaluated in this study. The effect of inhibitor B was dramatic. The inhibitor reduced the corrosion rate immediately upon injection. The same effect was observed in the single-phase flow loop study. The first inhibitor test was carried out at gas velocity of 23 m/s in the annular flow regime. Addition of 50 ppm of inhibitor B decreased the corrosion rate rapidly from 45 to 19 mpy in an hour. The corrosion rate was further decreased and stabilized at 14 mpy as time progressed. The calculated corrosion protection at 50 ppm was equivalent to 69%. The low corrosion protection at this concentration did not favor good corrosion protection at lower velocities where flow accelerated corrosion was more severe. Therefore, no further inhibitor testing was performed at this concentration (*i.e.*, 50 ppm).

As the concentration of inhibitor was increased to 100 ppm, the corrosion rate at 23 m/s gas velocity decreased quickly to 3 mpy after an hour. The corrosion rate decreased further to less than 2 mpy, which was the detection limit of the present measurement system. This is equivalent to in excess of 96% corrosion protection. It was deemed unnecessary to conduct further inhibitor evaluation at higher concentrations (i.e., 150 and 200 ppm) since corrosion was successfully inhibited at 100 ppm.

The results obtained at 15 m/s gas velocity were similar to those recorded at 23 m/s, likely due to the fact that both are in the annular flow regime. Addition of 100 ppm of inhibitor B decreased the corrosion rate from 67 to 6 mpy within an hour, and continued to decrease with time to below 2 mpy. Corrosion protection was greater than 97%. For the same reason as in the high gas velocity study (23 m/s), the inhibitor tests at 150 and 200 ppm were deemed unnecessary.

As the gas velocity was further decreased to 7.5 m/s, the corresponding flow regime changed to slug flow with a frequency of 4 to 6 slugs per minute passing down the test section. It is well known that slug flow gives the highest corrosion rate due to the high level of turbulence and localized shear forces at the front of each slug. As a consequence, pitting corrosion is quite typical for corrosion in slug flow. Presence of slug also increased the baseline corrosion rate to 105 mpy.

Injection of 100 ppm of inhibitor B to the loop reduced the corrosion rate from 105 to 23 mpy after an hour. The corrosion rate continued to decrease and eventually stabilized at 16 mpy. This amounts to 85% corrosion protection. As the concentration was further increased to 150 ppm, the corrosion rate was reduced to a final rate of 11 mpy, equivalent to 90% protection. No further decrease in corrosion rate was noted upon raising the inhibitor concentration to 200 ppm.

Corrosion and Inhibition Using De-ionized Water and Oil. Since the corrosion protection by inhibitor B were acceptable, it was decided to change the water composition from the synthetic brine to de-ionized water. This was to simulate the condition where water was mainly coming from condensation. The lack of buffering ions in the de-ionized water made the fluid more corrosive. In this series of tests, the pump was assembled with an undersized rotor to eliminate the abrasion problems of

rubber interior in the stator during high temperature operations. The change allowed tests to be conducted at 130°C. The same flow conditions as used in the previous tests with synthetic brine were used. Tests were carried out at both 95 and 130°C. The baseline corrosion rates are given in TABLE 4. The iron content for these tests was approximately 30 ppm.

TABLE 4. Baseline corrosion rates at 95°C and 130°C under 0.8 MPa CO_2 in multiphase flow containing 90% de-ionized water and 10% oil as liquid phase

Gas velocity m/s	Corrosion Rate at 95 C mpy	Corrosion rate at 130 C mpy
7.5	120	124
15	78	80
18	72	N/A
25	N/A[1]	60

1. Test was not performed due to high liquid slippage as a result of undersized rotor

The undersized rotor did cause some problems in experiments at 95°C. Since the rotor was smaller in diameter, the seal between the rotor and the stator was not perfectly tight. This led to significant gas slippage through the pump and, consequently, the highest gas velocity at 25 m/s could not be achieved. The maximum gas velocity for experiments at 95°C had to be limited to 18 m/s. Gas slippage, however, was not a problem for the experiments at 130°C. The seal was good and gas velocity of 25 m/s was attainable. As shown in TABLE 4, increasing the temperature from 95 to 130°C did not change the baseline corrosion rate substantially. The pH values for these runs were approximately 4.0. Inhibitor B was added at various concentrations to study the effectiveness of corrosion inhibitor. The results from the 95 and 130°C experiments are listed in TABLE 5 and 6, respectively. The experiment with 50 ppm of inhibitor B and 130°C was carried out first and it was found that 50 ppm was not sufficient to provide adequate corrosion protection. The result also agreed well with the previous tests at 95°C using the synthetic brine. Because of the low corrosion protection at 50 ppm from these previous experiments, it was decided to bypass the 50 ppm tests at 95°C and to jump directly to 100 ppm.

TABLE 5. Baseline and inhibited corrosion rates at 95°C and 0.8 MPa CO_2 in multiphase flow containing 90% de-ionized water and 10% oil as liquid phase

Gas velocity, m/s	Baseline corrosion rate, mpy	Corrosion rate, mpy @ 100 ppm	Protection @ 100 ppm	Corrosion rate, mpy @ 150 ppm	Protection @ 150 ppm
7.5	120	6	95%	6	95%
15	76	3	96%	< 2	> 97%

The results shown in TABLE 5 are comparable with those in TABLE 3. Tests in TABLE 3 were conducted with the use of synthetic brine whereas de-ionized water was used in the tests in TABLE 5. The percent protection looks slightly better in TABLE 5 than in TABLE 3. The difference is very trivial and is attributed to the high baseline corrosion rates in TABLE 5 in which de-ionized water was used. The inhibitor was very effective under all test conditions. Even in the most severe slug flow condition (at 7.5 m/s gas velocity), the corrosion rate could be reduced to 6 mpy at 100 ppm of inhibitor. However, further increasing the dosage did not reduce the corrosion rate significantly. With respect to

the annular flow condition (at 15 m/s gas velocity), the corrosion rate was reduced to less than 2 mpy at 150 ppm of inhibitor.

TABLE 6. Baseline and inhibited corrosion rates at 130°C and 0.8 MPa CO_2 in multiphase flow containing 90% de-ionized water and 10% oil as liquid phase

Gas velocity, m/s	Baseline CR#, mpy	CR#, mpy	P%*	CR#, mpy	P%*	CR#, mpy	P%*	CR#, mpy	P%*
Inhibitor, ppm	0	50		100		150		200	
7.5	125	18	86%	8	94%	6	95%	5	96%
15	80	11	86%	10	88%	< 2	> 97%	N/A	N/A
25	60	12	80%	8	87%	< 2	> 96%	N/A	N/A

CR = corrosion rate

* P% = percentage of corrosion protection

As stated earlier, the performance of 50 ppm of inhibitor B was marginal at 130°C. The corrosion protection was in the 80%'s regardless of gas velocity (or flow regime). However, increasing the inhibitor concentration to 100 ppm boosted the performance significantly. The corrosion rate at 7.5 m/s gas velocity decreased from 125 to 8 mpy, equivalent to 94% protection. The corrosion rates at 15 and 25 m/s gas velocities also decreased to 10 and 8 mpy, respectively. Further increasing the inhibitor concentration to 150 ppm improved the efficiency at 7.5 m/s gas velocity slightly, but did considerably reduce the corrosion rate at 15 and 25 m/s velocities to less than 2 mpy. The overall effectiveness was 95% for the 7.5 m/s gas velocity in slug flow and greater than 96% for the higher velocities in annular flow. Since over 95% corrosion protection was achieved at 150 ppm of inhibitor, very little improvement was noticed upon further increasing the dosage to 200 ppm.

It should be pointed out that the reported corrosion rates are those measured using conventional probes and only give an indication of general or uniform corrosion. In slug flow and in the presence of high concentration of chlorides, the main corrosion mechanism is pitting corrosion. Therefore, the localized corrosion rates are likely to be higher than those reported.

CONCLUSIONS

Flow loop experiments have been carried out under single-phase and multiphase conditions at a partial pressure of 0.7 - 0.8 MPa carbon dioxide and temperatures of 93 and 130°C. The highest liquid velocity considered in the single-phase flow loop was 14 m/s. The gas velocity in the multiphase flow loop was up to 25 m/s with the gas/oil ratio kept at 1780 sm^3/sm^3. Two flow regimes, annular and slug flow, were established in the multiphase flow loop under the conditions of interest.

Baseline corrosion rates were measured to determine the severity of corrosion. The performance of two corrosion inhibitors, specially formulated for high shear applications, was evaluated at concentrations in the range 50-200 ppm to assess their performance under varying flow conditions.

The measured baseline corrosion rates were higher in the single-phase flow loop than in the multiphase flow loop. The difference is attributed to the geometrical location of the probe in the single-

phase loop. A baseline corrosion rate of around 1500 mpy was measured in the high velocity section of this test assembly.

In comparison, the highest corrosion rate measured in the multiphase flow loop was 125 mpy, more than an order of magnitude lower than that observed in the single-phase flow loop.

The two specially formulated corrosion inhibitors evaluated were very effective over the range of flow conditions considered. A protective film formed almost instantaneously, as indicated by the rapid decrease in corrosion rate immediately upon injection of inhibitors. Effective protection was demonstrated at a corrosion inhibitor concentration of around 100 ppm.

This study indicates that corrosion inhibitors can satisfactorily mitigate corrosion in pipelines carrying wet, corrosive multiphase hydrocarbon product at high velocities. The results support the use of inhibitor and carbon steel as a viable combination for pipelines to be designed for a high production throughput. The combination can reduce the front-end capital cost considerably and offers a very attractive option for those fields having a short life or uncertain recoverable reserves.

UNIT GLOSSARY

ppb	part per billion	m/s:	meter per second
mpy:	mils per year	ppm:	part per million
L/s	liter per second	Pa	Pascal
sm^3	standard cubic meter	cP	centipoise
MPa	million Pascal		

ACKNOWLEDGEMENT

The authors would like to thank Antoine Griffin (Nalco/Exxon), Bruce Brown and Cheolho Kang (Ohio Univ.) for conducting the experiments reported in this paper. We would also like to thank our organizations for their permission to publish this work.

REFERENCES

1. Kapusta, S. D., Pots, B. F. M. and Connell, R. A., "*Corrosion Management of Wet Gas Pipelines*", paper no. 45, CORROSION/99, NACE International, 1999.

2. Attwood, P. A., Gelder, K. V. and Charmley, C. D., "*CO_2 Corrosion in Wet Gas Systems*", paper no. 32, CORROSION/96, NACE International, 1996.

3. Gunaltun, Y., Supriyatman, D. and Achmad, J., "*Top of the Line Corrosion in Multiphase Gas Line: A Case History*", paper no. 36, CORROSION/99, NACE International, 1999.

4. Schutt, H. U. and Lyle, F. F., "*CO_2/H_2S Corrosion Under Wet gas Pipeline Conditions in the Presence of Bicarbonate, Chloride and Oxygen*", paper no. 11, CORROSION/98, NACE International, 1998.

5. Jepson, W. P., Kaul, A. and Gopal, M., "*Mechanisms Contributing to Enhanced Corrosion in Three Phase Slug Flow in Multiphase Pipes*", paper no. 105, CORROSION/95, NACE International, 1995.

6. Jordan, K. G. and Rhodes, P. R., "*Corrosion of Carbon Steel by CO_2 Solution – The Role of Fluid Flow*", paper no. 125, CORROSION/95, NACE International, 1995.

7. Dugstad, A., "*Mechanism of Protective Film Formation During CO_2 Corrosion of Carbon Steel*", paper no. 31, CORROSION/98, NACE International, 1998.

8. Kvarekval, J.., "*Flow Loop Studies of the Relationship between Limiting Currents and CO_2/H_2S Corrosion of Carbon Steel*", paper no. 44, CORROSION/98, NACE International, 1998.

9. Fu, S. L. and Strickland, J. B., "*Corrosion Study in Dynamic High Velocity Flow Application Based on New Flow Loop Data*", paper no. 117, CORROSION/93, NACE International, 1993.

10. Chen, Y., Jepson, W. P. and Chen, H. J., "*Effect of Multiphase Flow on Corrosion Inhibitor*", paper no. 12, CORROSION/99, NACE International, 1999.

11. John, R., Jordan, K. G., Kapusta, S. D., Young, A. L. and Thompson, W. T., "*SweetCor: An Information System for the Analysis of Corrosion of Steels by Water and Carbon Dioxide*", paper no. 20, CORROSION/98, NACE International, 1998.

12. Kolts, J. Joosten, M. W., Humble, P. G. and Clapham, J., "*Aspects of Corrosion Inhibitor Selection at Elevated Temperatures*", paper no. 37, CORROSION/98, NACE International, 1998.

13. Kapusta, S. D., "*Corrosion Inhibitor Testing and Selection for Exploration and Production: A User's Perspective*", paper no. 16, CORROSION/99, NACE International, 1999.

14. Fu, S. L. and Bluth, M. J., "*Flow Enhanced Corrosion and Chemical Inhibition of Two-phase Brine and Hydrocarbon Flowing Systems*", paper no. 109, CORROSION/95, NACE International, 1995.

15. Kolts, J and Buck, E., "*Flow Effects in Corrosion Inhibitor Selection*", paper no. 108, CORROSION/95, NACE International, 1995.

16. Fu, S. L. and Bluth, M. J., "*A Statistical Study of Pipeline Corrosion in a High-Pressure Simulated Flow Loop*", Paper 7208, 25th Offshore Technology Conference, 1993.

17. Chen, H. J. and Jepson, W. P., "*Inhibition of Slug Front Corrosion in Multiphase Flow*", paper no. 54, CORROSION/98, NACE International, 1998.

18. Gopal, M. and Rajappa, S., "*Effect of Multiphase Slug Flow on the Stability of Corrosion Product Layer*", paper no. 46, CORROSION/99, NACE International, 1999.

19. "Design and Installation of *Offshore Production platform Piping Systems*", API-RP-14E, American Petroleum Institute, 1975.

20. Schmitt, G. and Mueller, M., "*Critical Wall Shear Stresses in CO_2 Corrosion of Carbon Steel*", paper no. 44, CORROSION/99, NACE International, 1999.

21. Shadley, J. R., Shirazi, S. A., Dayalan, E. and Rybicki, E. F, "*Velocity Guidelines for Preventing Pitting of Carbon Steel Piping When Flowing Medium Contains CO_2 and Sand*", paper no. 15, CORROSION/96, NACE International, 1996.

22. Jordan, K., "*Erosion in Multiphase Production of Oil and Gas*", paper no. 58, CORROSION/98, NACE International, 1998.

23. Colebrook, C. F., J. Inst. Civil Eng. (LONDON), **11**, pp. 133-156 (1938-1939).

24. Mansfeld, F., *"Polarization Resistance Measurement – Experimental Procedure and Evaluation of Test Data"*, Electrochemical Technique for Corrosion., Ed., Baboian, R., pp. 18 NACE International (1977).

25. Stern, M and Geary, A. L., *"Electrochemical Polarization. I. A Theoretical Analysis of the Shape of Polarization Curves"*, J. Electrochem. Soc., **104**, 33-63 (1957)1